



HAL
open science

A new method for determining $^{236}\text{U}/^{238}\text{U}$ isotope ratios in environmental samples by means of ICP-MS/MS

Silvia Diez-Fernández, Hugo Jaegler, Carole Bresson, Frédéric Chartier, O. Evrard, Amélie Hubert, Anthony Nonell, Fabien Pointurier, Hélène Isnard

► To cite this version:

Silvia Diez-Fernández, Hugo Jaegler, Carole Bresson, Frédéric Chartier, O. Evrard, et al.. A new method for determining $^{236}\text{U}/^{238}\text{U}$ isotope ratios in environmental samples by means of ICP-MS/MS. *Talanta*, 2020, 206, pp.120221. 10.1016/j.talanta.2019.120221 . cea-02610582

HAL Id: cea-02610582

<https://cea.hal.science/cea-02610582>

Submitted on 18 May 2020

HAL is a multi-disciplinary open access archive for the deposit and dissemination of scientific research documents, whether they are published or not. The documents may come from teaching and research institutions in France or abroad, or from public or private research centers.

L'archive ouverte pluridisciplinaire **HAL**, est destinée au dépôt et à la diffusion de documents scientifiques de niveau recherche, publiés ou non, émanant des établissements d'enseignement et de recherche français ou étrangers, des laboratoires publics ou privés.

1 A NEW METHOD FOR DETERMINING $^{236}\text{U}/^{238}\text{U}$ ISOTOPE RATIOS IN
2 ENVIRONMENTAL SAMPLES BY MEANS OF ICP-MS/MS

3 Silvia Diez-Fernández¹, Hugo Jaegler², Carole Bresson¹, Frédéric Chartier³, Olivier Evrard²,
4 Amélie Hubert⁴, Anthony Nonell¹, Fabien Pointurier⁴, Hélène Isnard^{1*}.

5 1. Den – Service d’Etudes Analytiques et de Réactivité des Surfaces (SEARS), CEA,
6 Université Paris-Saclay, F-91191, Gif sur Yvette, France

7 2. Laboratoire des Sciences du Climat et de l’Environnement (LSCE-IPSL), UMR 8212
8 (CEA/CNRS/UVSQ), Université Paris-Saclay, Gif-sur-Yvette, France

9 3. Den – Département de Physico-Chimie (DPC), CEA, Université Paris-Saclay, F-
10 91191, Gif sur Yvette, France

11 4. CEA, DAM, DIF, 91297 Arpajon, France

13 * Corresponding author: helene.isnard@cea.fr

15 *Journal : **Talanta**

16 **Keywords** : Uranium-236, ICP-MS/MS, spectral interferences, MC-ICP-MS, Fukushima,
17 environmental samples.

18 **Highlights** :

22 **Abstract:**

1
2
3 23 The $^{236}\text{U}/^{238}\text{U}$ isotope ratio is a widely used tracer, which provides information on source
4
5 24 identification for safeguard purposes, nuclear forensic studies and environmental monitoring.
6
7 25 This paper describes an original approach to determine $^{236}\text{U}/^{238}\text{U}$ ratios, below 10^{-8} , in
8
9
10 26 environmental samples by combination of ICP-MS/MS for $^{236}\text{U}/^{238}\text{U}$ ratio and multiple
11
12 27 collector ICPMS measurements for $^{235}\text{U}/^{238}\text{U}$ and $^{234}\text{U}/^{235}\text{U}$ isotope ratios.
13
14
15 28 Since the hydride form of UO^+ (UOH^+) is less prone to occur than UH^+ , we were focused on
16
17 29 the oxidised forms of uranium in order to reduce hydride based-interferences in ICPMS/MS.
18
19
20 30 Then, in-cell ion-molecule reactions with O_2 and CO_2 were assessed to detect the uranium
21
22 31 isotopes in mass-shift mode ($\text{Q1: U}^+ \rightarrow \text{Q2: UO}^+$). The performances in terms of UO^+
23
24 32 sensitivity and minimisation of hydride form of UO^+ were evaluated using five different
25
26
27 33 desolvating systems. The best conditions, using an Apex Ω or an Aridus system, produced
28
29 34 uranium oxide hydride rate ($^{235}\text{U}^{16}\text{O}^{16}\text{H}^+ / ^{235}\text{U}^{16}\text{O}^+$) of about 10^{-7} with O_2 in the collision cell.
30
31
32 35 The method was validated through measurements of two certified IRMM standards with
33
34 36 $^{236}\text{U}/^{238}\text{U}$ isotope ratio of 1.245×10^{-7} and 1.052×10^{-8} , giving results in agreement with
35
36
37 37 certified reference values. The relative standard deviations on seven independent
38
39 38 measurements for each standard were respectively of 1.5% and 6.2%. Finally, environmental
40
41
42 39 samples corresponding to sediments from the radioactive contamination plume emitted by the
43
44 40 Fukushima Daiichi Nuclear Power Plant accident were analysed after a well-established
45
46 41 uranium chemical separation procedure. $^{236}\text{U}/^{238}\text{U}$ atomic ratios between 1.5×10^{-8} and $7 \times 10^{-$
47
48
49 42 9 were obtained with a level accuracy lower than 20%.

45 1. Introduction

46 Uranium-236 with a half-life of 23.4 million years was produced by the $^{235}\text{U}(n,\gamma)$ and $^{238}\text{U}(n,3n)$
47 nuclear reactions in nuclear atmospheric weapons testings carried out between 1945 and 1980 [1, 2].

48 The atmospheric nuclear tests released ^{236}U which deposited on ground as aerosol particles; this is
49 referred to as global fallout, with the $^{236}\text{U}/^{238}\text{U}$ isotope ratio falling in the range of 10^{-7} - 10^{-9} [1].

50 Uranium-236 is also produced via thermal neutron captures on ^{235}U in nuclear power plants or in
51 nature. In the terrestrial environment, the $^{236}\text{U}/^{238}\text{U}$ ratio signatures fall in the range of 10^{-11} to 10^{-14} [3,
52 4]. In nuclear reactors, the isotopic composition of $^{236}\text{U}/^{238}\text{U}$ varies and atomic ratios as high as 10^{-3}
53 can be reached. In the case of nuclear power plant accidents, like Chernobyl or Fukushima Daiichi, hot
54 particles with such high ratios can be found in the environment [5, 6]. Given its potential variation
55 depending on the emission source, the $^{236}\text{U}/^{238}\text{U}$ isotopic ratio has been used in nuclear forensics,
56 nuclear safeguard and environmental monitoring studies [7-12] and it is now considered to be a new
57 tracer for oceanographic studies [13-15].

58 Since uranium-236 is present at ultra-trace level in environmental samples, inductively coupled
59 plasma mass spectrometry (ICP-MS) is a sensitive and versatile analytical technique to determine
60 $^{236}\text{U}/^{238}\text{U}$ isotope ratios [9, 10]. The major concern for determining $^{236}\text{U}/^{238}\text{U}$ isotope ratios in such
61 samples by ICP-MS is to implement a careful sample preparation and uranium purification procedure
62 to prevent matrix effects [17, 18] and to perform several corrections in relation to the very low
63 abundance of ^{236}U relative to ^{238}U and ^{235}U . The two major corrections concern 1) the formation of
64 polyatomic interferences such as $^{235}\text{U}^1\text{H}^+$ whose formation rate in the plasma, expressed as UH^+/U^+
65 ratio, is about 10^{-5} [19], and 2) the overlap of the tailings of ^{238}U and ^{235}U . However, the determination
66 of $^{236}\text{U}/^{238}\text{U}$ isotope ratios as low as 10^{-8} - 10^{-9} is not possible with single quadrupole ICP-MS or double
67 focusing ICP-MS mainly because the peak tailing of ^{238}U on the adjacent masses is not completely
68 removed [20]. ICPMS/MS instruments, commercialized since 2012, provide peak tailing effect far
69 lower than other type of instrument [21]. With this new technology, an additional quadrupole is
70 introduced in front of the collision-reaction cell as a first mass filter stage. The presence of two
71 quadrupoles allows to eliminate peak tailing effects from ^{238}U and ^{235}U . Furthermore, the mass-shift

72 mode, which consists in U reaction with O₂ in the cell to form UO⁺, allows to reduce by one order of
73 magnitude the polyatomic interferences due to hydride forms UOH⁺, because they are less prone to
74 occur than UH⁺ [19]. The potential of the ICP MS/MS technology to determine ²³⁶U/²³⁸U isotope ratios
75 has been addressed by Tanimizu *et al.* in synthetic samples, with ratios between 1 x 10⁻⁷ and 2 x 10⁻⁹
76 [19]. This technology has been further used to determine ²³⁶U/²³⁸U isotope ratios in soil samples
77 contaminated by the Fukushima Daiichi Nuclear Power Plant (FDNPP) accident, showing isotope
78 ratios between 3 x 10⁻⁷ and 4 x 10⁻⁸ with uncertainties between 20 and 50% [11, 22].

79 In this work, we present a new method to determine very low ²³⁶U/²³⁸U isotope ratios by ICP-MS/MS.
80 All analytical steps were validated and a comprehensive evaluation of the uncertainty budget was
81 performed. All uranium isotope ratios were determined with the best precision in environmental
82 samples, especially by MC-ICP-MS for ²³⁴U/²³⁵U and ²³⁵U/²³⁸U and by ICP-MS/MS for ²³⁶U/²³⁸U that
83 is below 10⁻⁸. Before measurements, the sample preparation and purification of uranium were carried
84 out using a well-established procedure [23]. The ²³⁴U/²³⁵U determined by MC-ICP-MS was used to
85 correct the mass bias and the bias between analog and pulse counting modes of the secondary electron
86 multiplier in the ICP-MS/MS instrument. The operating conditions to obtain the best performance in
87 term of sensitivity and minimisation of polyatomic interferences are detailed and discussed. Firstly,
88 the reaction profiles of O₂ and CO₂ with U in the Collision Reaction Cell (CRC) were evaluated
89 independently [24-26] and in combination with He in the cell. Secondly, five desolvating systems,
90 with and without gas in the cell, were compared on the basis of two criteria, i.e. uranium sensitivity
91 and uranium hydride formation rate. Thirdly, after determining the optimal parameters, the
92 methodology was validated by assessing the reproducibility and accuracy of the ²³⁶U/²³⁸U ratios (about
93 10⁻⁷ and 10⁻⁸) in two certified IRMM (Joint Research Center, Geel) reference materials. The
94 methodology was finally applied to analyse real samples, made of sediments collected in the Mano
95 Dam Reservoir, which drains a part of the main radioactive plume released by the Fukushima Daiichi
96 Nuclear Power Plant (FDNPP) accident.

98 2. Materials and methods

99 **2.1. Reagents, isotopic reference materials and samples**

1
2
3 100 We used ultrapure water (18.2 MΩ cm) from Millipore (Molsheim, France), and analytical grade
4
5 101 HNO₃ (67-69% purity) and HCl (32-35% purity) acids (“PlasmaPure Plus degree”) from SCP Science
6
7 102 (Courtaboeuf, France). Ultrapure Ar, O₂, CO₂, N₂ and He were purchased from Air Liquide. Two
8
9 103 certified isotopic reference materials of uranium, IRMM 184 and IRMM 075/5, were used to
10
11 104 determine precision and accuracy of the ²³⁶U/²³⁸U ratio, determined by ICP-MS/MS. These two
12
13 105 standards show ²³⁶U/²³⁸U ratios of 1.245±0.002 x10⁻⁷ (IRMM 184) and 1.0652±0.0008 x10⁻⁸ (IRMM
14
15 106 075/5). ²³⁵U/²³⁸U ratio of 0.0072623 ±0.0000022 from IRMM 184 was used to measure the mass bias
16
17 107 factor on MC-ICP-MS measurements. The standard solutions were prepared by evaporating aliquots
18
19 108 of stock solution and dissolving the dry extract in 2% HNO₃. An in-house natural uranium powder
20
21 109 (U₃O₈) was dissolved in 0.5 mol L⁻¹ HNO₃ to prepare a stock solution used for optimization of the
22
23 110 measurement methods by ICP-MS/MS. The environmental samples were selected from a sediment
24
25 111 core (~35 cm depth) collected in Hayama Lake, located 39 km from the northwest of FDNPP (Mano
26
27 112 Dam reservoir), as described in Jaegler *et al.* [23].
28
29
30
31

32 **Sample preparation and chemical treatment:** Around 5 g of each sample collected in selected
33
34 114 layers along the length of the sediment core were calcined and dissolved by several leaching-
35
36 115 evaporation cycles with 14 mol.L⁻¹ HNO₃, and a final step with a mixture of HNO₃ (67%) and 10
37
38 116 mol.L⁻¹ HCl (37%) in a molar ratio of 1/3. Samples were further filtrated and evaporated again to be
39
40 117 recovered in a solution of 8 M HNO₃, before uranium separation by ion exchange chromatography.
41
42 118 The uranium fraction was collected and purified by successively using a 20-ml-column filled with
43
44 119 AG1X8 anion-exchange resin, and a 2 mL-column filled with UTEVA extraction resin (100 – 150
45
46 120 mesh). The eluate was evaporated to dryness and recovered in a final solution of 2% HNO₃ to be
47
48 121 analysed with both ICP-MS instruments. A schematic diagram of the sample treatment protocol is
49
50 122 given in Figure S1 and detailed in a previous study [23].
51
52
53
54

55 123 Two solutions from the IRMM 075/5 standard (called SDC1 and SDC2) underwent the whole
56
57 124 procedure including dissolution and purification through the two steps of ion exchange
58
59
60
61
62
63
64
65

125 chromatography, while a third solution (called SC1) was only subjected to the two steps of liquid
126 chromatography. Seven procedural blanks were included in the analytical sessions.

127 **2.2. Instrumentation**

128 **ICP-MS/MS:** The $^{236}\text{U}/^{238}\text{U}$ ratio was determined with an ICP-MS/MS (Agilent 8800 ICP-QQQ,
129 Tokyo, Japan). The ICP-MS/MS was optimized daily using a solution containing 10 ng mL^{-1} of Li,
130 Co, Y, Ce, Tl and U in 2% HNO_3 . The operating conditions for the instrument are summarized in
131 **Table S1**. The dead time of the secondary electron multiplier detector for this instrument was precisely
132 evaluated at 32 ns with a method previously described [27].

133 *Sample introduction system:* Five desolvating systems associated to the ICP-MS/MS were
134 compared : i) an Aridus IITM from Cetac Technologies (Nebraska, USA) and various Apex systems
135 from Elemental Scientific (Nebraska, USA): ii) an Apex IRTM, iii) an Apex Ω TM, iv) an Apex HFTM
136 without desolvating membrane, and v) an Apex HFTM with a desolvation membrane, the Spiro TDM.
137 All the devices were used with a $120\text{ }\mu\text{L mL}^{-1}$ microconcentric PFA nebulizer (Elemental Scientific,
138 ESI, USA). When no desolvating system was implemented, a MicroMist concentric quartz nebulizer
139 (Agilent, California, USA) was used at a flow rate around $300\text{ }\mu\text{L mL}^{-1}$. The different desolvating
140 systems were compared with respect to several parameters: uranium sensitivity and uranium oxide
141 hydride rate. Before comparison, the nebulizer gas, N_2 flows and, in the case of membrane systems
142 (Apex Ω TM, Spiro TDM and Aridus IITM), sweep gas flows, were optimized daily with respect to the
143 Ce oxide formation (CeO/Ce ratio <0.05 %).

144 *Uranium reactivity evaluation:* The reactivity of U in the cell with two different oxidizing agents
145 (O_2 and CO_2) was evaluated with respect to sensitivity of UO^+ . Both pure gases were introduced using
146 the third cell gas entrance. A step of 2% for the cell gases was applied, ranging from 0 to 40%. The
147 role of He was evaluated by increasing the gas flow from 0 to 6 mL min^{-1} , with a 0.2 mL min^{-1} step,
148 using the corresponding entrance of the cell.

150 **MC-ICP-MS:** An MC-ICP-MS Neptune Plus™ (Thermo Scientific, Bremen, Germany) was also
151 employed to determine the $^{234}\text{U}/^{235}\text{U}$ and $^{235}/^{238}\text{U}$ ratios with a high level of precision. The relevant
152 operating conditions are given in **Table S1**. The samples were introduced into the plasma by means of
153 a “stable introduction system” (SIS) composed of a 100 $\mu\text{L mL}^{-1}$ microconcentric PFA nebulizer
154 (Elemental Scientific, Nebraska, USA) mounted on a tandem quartz spray chamber made of a double-
155 pass chamber composed of cyclonic and Scott chambers, and equipped with a PC³ Peltier chiller
156 (Elemental Scientific, Nebraska, USA). The sensitivity was daily optimized to obtain a signal with
157 maximal intensity and stability.

158 **2.3. Analytical approach**

159 **Analytical method for MC-ICP-MS:** $^{235}\text{U}/^{238}\text{U}$ and $^{234}\text{U}/^{235}\text{U}$ isotope ratios were determined by MC-
160 ICP-MS. The sensitivity was around 125 V per ppm for U during the analytical sessions; the
161 acquisition method consisted of 30 cycles (3 blocks of 10 cycles) with an integration time of 4.2 s and
162 removal of outliers using a 2σ test. The instrumental mass bias was corrected by means of a classical
163 Sample Standard Bracketing (SSB) approach using the certified IRMM 184 standard and applying an
164 exponential law [28]. Concentrations of samples and standards were in the same range (less than 20%
165 relative difference between them). The analyses were conducted at low mass resolution and in static
166 mode. Signals for ^{235}U and ^{238}U isotopes were acquired using a Faraday cup equipped with 10^{11} Ohm
167 resistor amplifiers. The ^{234}U signal was acquired using a SEM detector combined with a Retarding
168 Potential Quadrupole (RPQ) to reduce abundance sensitivity. The SEM/Faraday yield was determined
169 by standard bracketing with the same IRMM 184 standard used for mass bias correction. By applying
170 this approach, the standard deviation obtained for the $^{234}\text{U}/^{238}\text{U}$ ratio was around 0.4% at $k=1$.
171 Uncertainties on $^{235}\text{U}/^{238}\text{U}$ and $^{234}\text{U}/^{235}\text{U}$ isotope ratios were calculated according to the Kragten
172 method, described elsewhere [29, 30].

173 **Analytical method for ICP-MS/MS:** All isotopes of uranium were measured in their corresponding
174 oxide forms (U^{16}O^+), taking advantage of the *mass-shift* mode [19]. Transitions are given in **Table S2**.
175 The $^{236}\text{U}/^{238}\text{U}$ ratio was determined indirectly by determining the $^{236}\text{U}/^{235}\text{U}$ ratio by ICP-MS/MS and

176 the $^{235}\text{U}/^{238}\text{U}$ ratio by MC-ICP-MS, in order to protect the detector from a too high $^{238}\text{UO}^+$ count rate
177 (10^9 counts. s^{-1}) and to obtain the lower uncertainty on all uranium isotope ratios.

178 The intensity of $^{234}\text{U}^{16}\text{O}^+$ and $^{236}\text{U}^{16}\text{O}^+$ signals was measured in pulse counting mode, while $^{235}\text{U}^{16}\text{O}^+$
179 and $^{238}\text{U}^{16}\text{O}^+$ were measured in analog mode. A total of 20 replicates were acquired for $^{234}\text{U}^{16}\text{O}^+$,
180 $^{235}\text{U}^{16}\text{O}^+$ and $^{236}\text{U}^{16}\text{O}^+$. $^{236}\text{U}^{16}\text{O}^+$ counting was also corrected from the formation of $^{235}\text{U}^{16}\text{O}^1\text{H}^+$. The
181 uranium oxide hydride formation rate was calculated in a separate acquisition method by determining
182 the $^{238}\text{U}^{16}\text{O}^1\text{H}^+/^{238}\text{U}^{16}\text{O}^+$ ratio. The method consisted of 5 replicates with 3 points per peak and 100
183 sweeps. Instrumental blanks were corrected for all U isotopes.

184 Experimental $^{236}\text{U}/^{235}\text{U}$ ratios were internally corrected in terms of the mass bias and the bias
185 corresponding to the combined pulse counting and analog detection modes. This “B” value was
186 calculated for the experimental $^{234}\text{U}/^{235}\text{U}$ ratio in each sample, following Eq (1):

$$B = \frac{\text{Ln}\left(\frac{\left(\frac{^{234}\text{U}}{^{235}\text{U}}\right)_{tr}}{\left(\frac{^{234}\text{U}}{^{235}\text{U}}\right)_{exp}}\right)}{\text{Ln}\left(\frac{m_{234}}{m_{235}}\right)}, \text{ (Eq. 1)}$$

187 where $(^{234}\text{U}/^{235}\text{U})_{tr}$ represents the true value of the ratio, $(^{234}\text{U}/^{235}\text{U})_{exp}$ represents the ratio obtained by
188 ICP-MS/MS, and m_{234} and m_{235} correspond to the exact mass of isotopes ^{234}U and ^{235}U respectively.

189 The true value of the $^{234}\text{U}/^{235}\text{U}$ ratio in the IRMM 184 is the certified one, while this ratio was
190 measured by MC-ICP-MS for IRMM 075/5 and for the samples. Once the experimental ratio $^{236}\text{U}/^{235}\text{U}$
191 had been corrected with the B value, the final $^{236}\text{U}/^{238}\text{U}$ ratios in the samples were calculated by
192 multiplying the corrected $^{236}\text{U}/^{235}\text{U}$ ratios by the $^{235}\text{U}/^{238}\text{U}$ values, previously determined by MC-ICP-
193 MS. Uncertainties were calculated according to the Kragten method [29, 30].

195 3. Results and discussion

196 3.1. Study of gas reactivity and collisional focusing

197 One of the main concerns with respect to determining the $^{236}\text{U}/^{238}\text{U}$ ratio in environmental samples is
198 the formation of $^{235}\text{U}^1\text{H}$ ($m/z=236$) in the plasma. To correct this interference, the $^{238}\text{UH}^+/^{238}\text{U}^+$ ratio in

199 our instrument in a single quadrupole mode and in a standard configuration without desolvating
200 system, was measured around 7×10^{-5} , which is in agreement with values quoted in the literature [11,
201 23]. This hydride formation is not negligible considering that the $^{236}\text{U}/^{235}\text{U}$ ratios in our IRMM
202 standards are below 10^{-5} , and also expected in the samples. As described by Tanimizu *et al.* [19], the
203 collision/reaction technology made possible by ICP-MS/MS, allows to reduce such rate thanks to the
204 *mass-shift* mode, through the reaction of U with O_2 in the cell to form UO^+ ($\text{U}^+ + \text{O}_2 \rightarrow \text{UO}^+ + \text{O}$, $\Delta H_r =$
205 -2.89 eV). This reduces hydride based-interferences compared with the SQ mode, since the hydride
206 form of UO^+ (UOH^+) is less prone to occur than UH^+ .

207 Using this method, two different oxidizing agents were compared as cell gases (O_2 and CO_2) in order
208 to provide the best performance in term of sensitivity for signal of oxide form of uranium. Reaction
209 curves, corresponding to the variations of the signal intensity of the oxide form of uranium as a
210 function of the gas flow introduced in the cell, were plotted for a $0.050 \mu\text{g mL}^{-1}$ U solution (Figure 1).
211 As can be observed, both reaction profiles are similar in shape and sensitivity ($\sim 9 \times 10^5$ counts. s^{-1} for
212 $^{238}\text{UO}^+$), although the optimal gas flow for CO_2 is slightly shifted with respect to O_2 (10% and 7%
213 respectively). The total oxide rate conversion could not be computed since UO^+ oxide reacts with O_2
214 to form UO_2^+ ($\Delta H_r = -2.63$ eV) at m/z 270, being outside the recording range of the instrument
215 (maximum m/z at 260). Potential collisional focusing effects already described in the literature [31]
216 were also evaluated by adding He in the cell along with the corresponding reaction gas (O_2 , CO_2).
217 Since no sensitivity enhancement was observed (Figure S2), He was no longer used. This may be
218 related to the fact that O_2 and CO_2 already produce some collisional focusing; not only inelastic
219 collisions occur, leading to the formation of the expected ion, but also elastic collisions for which there
220 is no energy exchange and thus no reaction. According to these results, the reaction gas of choice was
221 O_2 , since CO_2 does not improve either or UO^+ sensitivity or the formation of UOH^+ .

3.2. Uranium oxide hydride formation rate using different desolvating systems

223 Although the *mass-shift* strategy can reduce the uranium oxide hydride formation rate to around one
224 order of magnitude, it remains necessary to reduce its incidence over ^{236}U to reach the desired ratios.
225 Consequently, the following step was to access the different desolvating devices described in section

226 2.2. Such sample introduction systems are able to remove the solvent from the matrix and decrease the
1 hydride formation [32]. Comparisons were performed on the basis of the sensitivity at $m/z = {}^{238}\text{U}^{16}\text{O}^+$
2
3
4 228 and the uranium oxide hydride formation rate (${}^{238}\text{UOH}^+ / {}^{238}\text{UO}^+$), using a $1 \mu\text{g mL}^{-1}$ U solution. In each
5
6 229 analytical session, the carrier gas and the N_2 flows were optimised for all the systems in order to
7
8 230 provide the best conditions, as was the Ar sweeping gas flow for the Apex HF+Spiro, Apex Ω and
9
10 231 Aridus systems. Considering the instrumental variation from day to day, the sensitivity values in **Table**
11
12 232 **1** are mostly given as a range. In the configuration, without a desolvating system and in MS/MS mode,
13
14 233 the sensitivity was around $100,000 \text{ counts}\cdot\text{s}^{-1}$ per ng mL^{-1} for ${}^{238}\text{UO}^+$, and the ${}^{238}\text{UOH}^+ / {}^{238}\text{UO}^+$ ratio
15
16 234 was 3×10^{-6} . The Apex IR system provided a slight improvement in sensitivity, though the uranium
17
18 235 oxide hydride formation rate remained unchanged. This may be due to the system design, focused on
19
20 236 providing high reproducibility for isotope ratio determination. Although the sensitivity increased by a
21
22 237 factor two with the Apex HF, the uranium oxide hydride formation rate remained also unchanged. The
23
24 238 addition of the Spiro TDM membrane to the Apex HF did not allow the reduction of the ${}^{238}\text{UOH}^+$
25
26 239 formation rate. Best results were obtained with the Aridus and the Apex Ω systems. Representative
27
28 240 operating conditions for these two systems are given in **Table S3**. Sensitivity increased around 4 fold,
29
30 241 while the uranium oxide formation hydride rate decreased by one order of magnitude, down to 3×10^{-7}
31
32 242 (${}^{238}\text{U}^{16}\text{O}^1\text{H}^+ / {}^{238}\text{U}^{16}\text{O}^+$). However, the stabilization time required to attain the adequate hydride rate
33
34 243 using the APEX Ω system was significantly shorter than this needed for the ARIDUS system. Both
35
36 244 desolvating systems were used in the rest of the study.
37
38
39
40
41
42

43 245 **3.3. Abundance sensitivity**

44
45 246 The effect of ${}^{238}\text{U}$ tailing over the minor ${}^{236}\text{U}$ isotope has been described for numerous sample
46
47 247 introduction systems with respect to determining ${}^{236}\text{U} / {}^{238}\text{U}$ ratios [33]. Reported values of abundance
48
49 248 sensitivity for a standard ICP-QMS instrument tend to be about 10^{-6} , however two quadrupoles
50
51 249 positioned in a tandem configuration provided abundance sensitivity values between 10^{-10} and 10^{-14}
52
53 250 [21], which would virtually allow to determine very low ratios. In our case, the abundance sensitivity
54
55 251 was estimated below 10^{-9} in MS/MS mode, considering the contribution of ${}^{238}\text{U}^{16}\text{O}^+$ at $m/z = 253$. An
56
57 252 accurate measurement of the contribution of the ${}^{238}\text{U}$ tailing at the ${}^{236}\text{U}$ m/z is limited by the dynamic
58
59
60
61
62
63
64
65

253 range of the detector (10^{10}). In order to evaluate this contribution, a 500 ng mL^{-1} solution of natural U
1
2 254 in 2% HNO_3 with ^{236}U abundance lower than 10^{-10} was analysed in SQ and MS/MS modes. Mass
3
4 255 spectra were recorded from $m/z = 234$ to $m/z = 239$ in SQ mode, while they were recorded between
5
6 256 $m/z = 250$ and $m/z = 255$ in MS/MS mode. Masses at $m/z = 239$ in SQ mode and $m/z = 255$ in MS/MS
7
8 257 mode were included in order to observe the uranium hydride and uranium oxide hydride ($^{238}\text{U}^1\text{H}^+$ and
9
10 $^{238}\text{U}^{16}\text{O}^1\text{H}^+$, respectively). Both spectra are shown in **Figure 2**. As can be seen, peaks in the spectrum
11 258 registered in SQ mode overlap completely. Peaks observed at $m/z = 237$ are due to a significant ^{238}U
12
13 259 peak tailing effect and peaks at $m/z=236$ corresponds to ^{238}U tailing and $^{235}\text{UH}^+$. It is also worth noting
14
15 260 the decrease in the uranium hydride formation rate when switching from SQ mode to MS/MS mode,
16
17 261 as already explained. Analysis in MS/MS mode completely removes the tailing effects, according to
18
19 262 the peaks shapes shown in **Figure 2**.
20
21
22 263

25 264 **3.4. Isotope ratio measurements in standards**

27 265 **3.4.1. Non-treated standards**

26 266 Accuracy and reproducibility of the $^{236}\text{U}/^{235}\text{U}$ ratio measurements with ICP-MS/MS was checked by
27
28 267 the analysis of two certified standards: IRMM 184 and IRMM 075/5. These two standards were
29
30 268 specifically chosen because of their $^{236}\text{U}/^{238}\text{U}$ ratios, close to those expected in the samples:
31
32 269 $1.245 \pm 0.002 \times 10^{-7}$ (IRMM 184) and $1.0652 \pm 0.0008 \times 10^{-8}$ (IRMM 075/5). Whereas all uranium
33
34 270 isotope ratios are certified for the IRMM 184 standard ($^{234}\text{U}/^{235}\text{U} = 0.007317 \pm 0.000005$;
35
36 271 $^{235}\text{U}/^{238}\text{U} = 0.0072623 \pm 0.000002$), only the $^{236}\text{U}/^{238}\text{U}$ ratio is certified for IRMM 075/5. Therefore, the
37
38 272 "reference" $^{235}\text{U}/^{238}\text{U}$ and $^{234}\text{U}/^{235}\text{U}$ ratios were determined by MC-ICP-MS. For this, three solutions of
39
40 273 IRMM 075/5 containing 200 ng mL^{-1} of U were analysed as explained in previous sections. Average
41
42 274 values obtained for the $^{234}\text{U}/^{235}\text{U}$ and $^{235}\text{U}/^{238}\text{U}$ ratios were 0.007332 ± 0.000005 ($n=3$) and 0.0072575
43
44 275 ± 0.0000009 ($n=3$) respectively. For our purposes, these values were used as references to correct the
45
46 276 experimental $^{236}\text{U}/^{235}\text{U}$ ratios obtained by ICP-MS/MS.
47
48
49
50
51
52
53

54
55 277 The $^{236}\text{U}/^{235}\text{U}$ ratio was determined for both standards in seven solutions, each containing around $1 \mu\text{g}$
56
57 278 mL^{-1} of U, with the ICP-MS/MS equipped with an Aridus desolvating system. Experimental ratios
58
59 279 were individually calculated using the corresponding B value for mass and detector bias corrections.
60
61
62
63
64
65

280 The contribution of $^{235}\text{U}^{16}\text{O}^+\text{H}^+$ and of the instrumental blanks over $^{236}\text{U}^{16}\text{O}^+$ were subtracted at $m/z =$
281 252 ($^{236}\text{UO}^+$). Final $^{236}\text{U}/^{238}\text{U}$ ratios for the IRMM 184 and IRMM 075/5 standards are shown in
282 **Tables 2 and 3** respectively.

283 Regarding IRMM 184, uncertainties for the $^{236}\text{U}/^{238}\text{U}$ ratios were between 2-3% in most cases. The
284 $^{236}\text{U}/^{238}\text{U}$ ratios obtained for seven standard solutions analysed during different analytical sessions,
285 showed a relative standard deviation of 1.5%, lower than the calculated uncertainties. The accuracy of
286 the average value with respect to the certified ratio was -0.6%. A similar situation was found for the
287 IRMM 075/5. However, uncertainties were much more variable, ranging between 8-23%, because of
288 the very low counting for the $^{236}\text{UO}^+$ signal. In any case, the relative standard deviation between the
289 seven different measurements was 6.2%, lower than the uncertainty. Accuracy for the average value
290 was 2.6%.

3.4.2. Treated standards

292 To make sure that ^{236}U cannot be polluted during the chemical pre-treatment of the samples, three
293 solutions of the IRMM 075/5 standard – called SC1, SDC1 and SDC2 were also subjected to the
294 chemical separation and purification procedure. Along with the standards, three procedural blanks
295 were included in the analytical session. For the analysis of these samples, the desolvating Apex Ω
296 system was used.

297 The signal at $^{236}\text{U}^{16}\text{O}^+$ m/z in the three procedural blank solutions showed counting lower than 0.2 cps.
298 By contrast, the absolute count rates of the standard solutions for the same $^{236}\text{U}^{16}\text{O}^+$ signal was around
299 10 cps, meaning that the contribution of the blank was less than 2% of the final $^{236}\text{U}^{16}\text{O}^+$ signal and
300 can therefore be neglected.

301 As for the non-treated standards, the $^{234}\text{U}/^{235}\text{U}$ and $^{235}\text{U}/^{238}\text{U}$ ratios were determined by MC-ICP-MS.
302 Average values were 0.007336 ± 0.000012 and 0.0072566 ± 0.0000011 for $^{234}\text{U}/^{235}\text{U}$ and $^{235}\text{U}/^{238}\text{U}$
303 ratios respectively. These values are statistically indistinguishable from those obtained for the non-
304 treated standards ($^{234}\text{U}/^{235}\text{U}=0.007332 \pm 0.000005$; $^{235}\text{U}/^{238}\text{U}=0.0072575 \pm 0.0000009$).

305 With respect to the $^{236}\text{U}/^{238}\text{U}$ ratio, and considering the lower precision of the measurements
1
2 306 performed by ICP-MS/MS, three non-treated IRMM 075/5 standards (I, II, III) were also measured
3
4 307 before and after the treated standards. The results are given in **Figure 3**. The average $^{236}\text{U}/^{238}\text{U}$ ratio for
5
6 308 non-treated standards was $1.10 \pm 0.03 \times 10^{-8}$, statistically similar to this measured for the treated
7
8 309 standards ($1.13 \pm 0.10 \times 10^{-8}$ for SC1 and $1.11 \pm 0.03 \times 10^{-8}$ for SCD1 and SCD2). Consequently, no
9
10
11 310 detectable differences in isotope ratios due to the sample treatment procedure could be found.
12

14 311 *3.4.3. Assessing sources of uncertainty*

16 312 The Kragten method provides information on the relative contribution of each error source on the final
17
18 313 uncertainty. Error sources taken into account are: count rates at the different m/z in samples and blank
19
20 314 solutions, uncertainties on the certified ratios of the isotope standards. As an example, the relative
21
22 315 contribution of each source on the final uncertainty is shown in **Table 4**. As can be observed, more
23
24 316 than 90% of the uncertainty budget is due to $^{236}\text{U}^{16}\text{O}^+$ count rate, which, as mentioned before, is
25
26 317 around 10 cps for the IRMM 075/5 standard at $1 \mu\text{g mL}^{-1}$ U. Other significant contributions were the
27
28 318 count rates for $^{238}\text{U}^{16}\text{OH}^+$ and $^{235}\text{U}^{16}\text{O}^+$ with 6.6% and 1.1% respectively. The influence of the other
29
30 319 terms tended to be minor, mostly below 0.5%.
31
32
33
34
35 320

37 321 *3.5. Isotope ratio measurements in the Fukushima environmental samples.*

38
39 322 The $^{235}\text{U}/^{238}\text{U}$ and $^{234}\text{U}/^{235}\text{U}$ ratios were measured by MC-ICP-MS, and the $^{236}\text{U}/^{235}\text{U}$ ratio was
40
41 323 measured by ICP-MS/MS using an Aridus system. Solutions were diluted to obtain a final U
42
43 324 concentration of around $1 \mu\text{g mL}^{-1}$ to ensure that the $^{236}\text{U}^{16}\text{O}^+$ counting rate would be detectable.
44
45

46 325 A 2% HNO_3 solution corresponding to the instrumental blank was analysed before each procedural
47
48 326 blank or sample. Corresponding counting rates at m/z of $^{236}\text{U}^{16}\text{O}^+$ for both types of blanks are shown in
49
50
51 327 **Figure 4**. There is no evidence of carry-over for the instrumental blank, as the counting remained
52
53 328 constant during the session. Besides, no significant differences were observed between the
54
55 329 instrumental (<0.4 cps) and the procedural blank (<0.7 cps), meaning that the sample treatment did not
56
57 330 contribute significantly to the $^{236}\text{U}^{16}\text{O}^+$ background.
58
59
60
61
62
63
64
65

331 Seven sections from a sediment core of the Mano Dam reservoir were analysed according to the
332 methodology described above. MDh corresponds to the sample closest to the surface, and MDb to the
333 deepest one. Set-up stability was checked before analysis through the analysis of standards. The
334 $^{234}\text{U}/^{235}\text{U}$ and $^{235}\text{U}/^{238}\text{U}$ ratios obtained by MC-ICP-MS, and $^{236}\text{U}/^{238}\text{U}$ ratios obtained by ICP-MS/MS
335 are given in **Table 5**. $^{234}\text{U}/^{235}\text{U}$ ratios were used for correction of $^{236}\text{U}/^{235}\text{U}$ ratios determined with ICP-
336 MS/MS. $^{235}\text{U}/^{238}\text{U}$ ratios were used for the final computation of the $^{236}\text{U}/^{238}\text{U}$ ratios. The average value
337 obtained for the $^{235}\text{U}/^{238}\text{U}$ ratio, i.e. 0.007257 ± 0.000003 , is in perfect agreement with the natural ratio
338 reported in the literature, i.e. 0.007257 ± 0.000004 [4]. Nonetheless, $^{234}\text{U}/^{235}\text{U}$ ratios vary slightly
339 between samples with a relative standard deviation of 2%. Uncertainties calculated for the samples
340 measured by ICP-MS/MS were consistent with the uncertainties obtained for the standards.
341 Measured $^{236}\text{U}/^{238}\text{U}$ ratios ranged between 7.0×10^{-9} and 4.2×10^{-8} . Associated uncertainties obtained
342 using the Kragten method varied between 6.7% and 16.8% at $k=2$. These values are significantly
343 lower than the uncertainties reported in previous publications using ICP-MS/MS technology for the
344 analysis of seawater and soil samples [11, 19, 21]. In the present work, the $^{236}\text{U}/^{238}\text{U}$ ratios measured
345 in sediments can be attributed to the global fallout values $<10^{-7}$ [23].

346 4. Conclusion

347 In this work, we present a new methodology to determine all uranium isotope ratios in environmental
348 samples after a chemical separation procedure involving a combination of anion exchange and
349 extraction resins. $^{234}\text{U}/^{238}\text{U}$ and $^{235}\text{U}/^{238}\text{U}$ ratios were determined by MC-ICP-MS while $^{236}\text{U}/^{238}\text{U}$
350 isotope ratios, which are below 10^{-8} , were measured using ICP-MS/MS. In this later case, the strategy
351 was based on the use of MS/MS mass-shift mode, since abundance sensitivity values are generally
352 below 10^{-10} and the hydride form of UO^+ (UOH^+) is less prone to occur than UH^+ . The selected gas
353 introduced in the cell was O_2 and in order to obtain the lower UOH^+/UO^+ ratio, five different
354 desolvating systems are tested. The Apex Ω and Aridus systems provided the best results in term of
355 sensitivity and UOH^+/UO^+ ratios down to 4×10^{-7} were reached.

356 The method was developed and validated for two certified IRMM isotopic standards with $^{236}\text{U}/^{238}\text{U}$
357 certified ratio of 1.245×10^{-7} (IRMM 184) and 1.052×10^{-8} (IRMM 075/5). The IRMM 075/5 standard

358 was subjected to the preparation and chemical purification procedure, and no detectable difference in
1
2 359 isotope ratios due to sample treatment was found. The isotopic ratios obtained for seven independent
3
4 360 measurements of the two standards gave results in agreement with certified reference values, with
5
6 361 relative standard deviation of respectively 1.5% (IRMM 184) and 6.2% (IRMM 075/5). Finally, the
7
8 362 $^{236}\text{U}/^{238}\text{U}$ isotope ratios were determined in sediments collected along a core in a lake draining a part
9
10
11 363 of the main radioactive pollution plume released by the FDNPP accident. The measured $^{236}\text{U}/^{238}\text{U}$
12
13 364 ranged between 7.0×10^{-9} and 4.2×10^{-8} , with accuracy levels below 20%, corresponding to the global
14
15 365 fallout signature. These ratios were the lowest ever measured by ICP-MS/MS in sediment samples,
16
17 366 with uncertainty below 20% for ratios below 10^{-8} .

20 367 **5. Acknowledgements**

23 368 The collection and analysis of the sediment samples were funded under the TOFU (ANR-11-JAPN-
24
25 369 001) and the AMORAD (ANR-11-RSNR-0002) projects, via by the French National Research Agency
26
27 370 (ANR).
28
29
30
31
32
33
34
35
36
37
38
39
40
41
42
43
44
45
46
47
48
49
50
51
52
53
54
55
56
57
58
59
60
61
62
63
64
65

- 371 [1] A. Sakaguchi, K. Kawai, P. Steier, F. Quinto, K. Mino, J. Tomita, M. Hoshi, N. Whitehead, M.
1 Yamamoto, First results on ^{236}U levels in global fallout. *Sci. Total Environ.* 407 (2009) 4238–4242.
2
3
4 373 DOI: 10.1016/j.scitotenv.2009.01.058.
5
6
7 374 [2] S.R. Winkler, P. Steier, J. Carilli, Bomb fall-out ^{236}U as global oceanic tracer using an annually
8
9 375 resolved coral core. *Earth Planet. Sci. Lett.* 359-360 (2012) 124-130. DOI: 10.1016/j.epsl.2012.10.004
10
11
12 376 [3] P. Steier, M. Bichler, L.K. Fifield, R. Golser, W. Kutschera, A. Priller, F. Quinto, S Richter, M.
13
14 377 Srncik, P. Terrasi, L. Walker, A. Wallner, G. Wallner, K.M. Wilcken, E.M. Wild, Natural and
15
16 378 anthropogenic ^{236}U in environmental samples. *Nucl. Instr. Meth. B* 266 (2008) 2246-2250. DOI:
17
18 379 10.1016/j.nimb.2008.03.002
19
20
21
22 380 [4] S. Richter, A. Alonso, W. De Bolle, R. Wellum, P.D.P. Taylor, Isotopic “fingerprint” for natural
23
24 381 uranium samples. *Int. J. Mass Spectrom.* 193 (1999) 9-14. DOI: 10.1016/S1387-3806(99)00102-5
25
26
27 382 [5] S.F. Boulyga, J.S. Becker, Determination of uranium isotopic composition and ^{236}U content of soil
28
29 383 samples and hot particles using inductively coupled plasma mass spectrometry. *Fresenius J. Anal.*
30
31 384 *Chem.* 30 (2001) 612-617. DOI 10.1007/s002160100838
32
33
34 385 [6] B. Salbu, L. Skipperud, O.C. Lind, Sources contributing to radionuclides in the environment: With
35
36 386 focus on radioactive particles. In: Walther C., Gupta DK, editors. *Radionuclides in the environment:*
37
38 387 *influence of chemical speciation and plant uptake on radionuclides migration.* Springer International
39
40 388 Publishing, p 1-36.
41
42
43
44 389 [7] R. Eigl, M. Srncik, P. Steier, G. Wallner, $^{236}\text{U}/^{238}\text{U}$ and $^{240}\text{Pu}/^{239}\text{Pu}$ isotopic in small (2L) sea and
45
46 390 river water samples. *J. Environ. Radioact.* 116 (2013) 54-58. DOI: 10.1016/j.jenvrad.2012.09.013
47
48
49 391 [8] F. Quinto, P. Steier, G. Wallner, A. Wallner, M. Srncik, M. Bichler, W. Kutschera, F. Terrasi, A.
50
51 392 Petraglia, C. Sabbarese, The first use of ^{236}U in the general environment and near a shutdown nuclear
52
53 393 power plant. *Appl. Radiat. Isotopes* 67 (2009) 11775-1780. DOI: 10.1016/j.apradiso.2009.05.007.
54
55
56
57
58
59
60
61
62
63
64
65

- 394 [9] S.F. Boulyga, J.S. Becker, J.L. Matusevitch, H-J. Dietze, Isotope ratio measurements of spent
1 reactor uranium in environmental samples by using inductively coupled plasma mass spectrometry.
2 395
3
4 396 Int. J. Mass Spectrom. 203 (2000) 143–154. DOI: 10.1016/S1387-3806(00)00296-7.
5
6
7 397 [10] J.S. Santos, L.S.G. Teixeira, W.N.L. dos Santos, V.A. Lemos, J.M. Godoy, S.L.C. Ferreira,
8
9 398 Uranium determination using atomic spectrometric techniques: An overview. Anal. Chim. Acta 674
10
11 399 (2010) 143-156. DOI: 10.1016/j.aca.2010.06.010.
12
13
14 400 [11] G. Yang, H. Tazoe, M. Yamada, Determination of ^{236}U in environmental samples by single
15
16 401 extraction chromatography coupled to triple-quadrupole inductively coupled plasma-mass
17
18 402 spectrometry. Anal. Chim. Acta 944 (2016) 44-50. DOI: 10.1016/j.aca.2016.09.033.
19
20
21
22 403 [12] W. Bu, J. Zheng, M.E. Ketterer, S. Hu, S. Uchida, X. Wang, Development and application of
23
24 404 mass spectrometric techniques for ultra-trace determination of ^{236}U in environmental samples-A
25
26 405 review. Analyt. Chim. Acta 995 (2017) DOI: 1-20. 10.1016/j.aca.2017.09.029
27
28
29 406 [13] M. Christl, C. Lachner, C. Vockenhuber, O. Lechtenfeld, I. Stimac, M.R. Van der Loeff, H.A.
30
31 407 Synal, A depth profile of uranium-236 in the Atlantic ocean. Geoch. Cosmochim. Acta 777 (2012) 98-
32
33 408 107. DOI: 10.1016/j.gca.2011.11.009
34
35
36 409 [14] R. Tortorello, E. Widom, W.H. Renwick, Use of uranium isotopes as a temporal and spatial tracer
37
38 410 of nuclear contamination in the environment. J. Environ. Radioact. 124 (2013) 287-300. DOI:
39
40 411 10.1016/j.jenvrad.2013.06.007
41
42
43
44 412 [15] A. Sakaguchi, T. Nomura, P. Steier, R. Golser, K. Sasaki, T. Watanabe, T. Nakakuki, Y.
45
46 413 Takahashi, H. Yamamo, Temporal and vertical distributions of anthropogenic ^{236}U in the Japan Sea
47
48 414 using a coral core and seawater samples. J. Geophys. Res. Oceans 121 (2016) 4-13. DOI:
49
50 415 10.1002/2015JC011109
51
52
53
54 416 [16] N. Casacuberta, M. Christl, J. Lachner, M.R. van der Loeff, P. Masque, H.A. Synal, A first
55
56 417 transect of ^{236}U in the North Atlantic ocean. Geoch. Cosmochim. Acta 133 (2014) 34-46. DOI:
57
58 418 10.1016/j.gca.2014.02.012
59
60
61
62
63
64
65

- 1
2 420 [17] E.P. Horwitz, M.L. Dietz, R. Chiarizia, H. Diamond, Separation and preconcentration of uranium
3
4 421 from acidic media by extraction chromatography. *Anal. Chim. Acta* 266 (1992) 25-37. DOI:
5
6 10.1016/0003-2670(92)85276-C
- 7 422 [18] J. Qiao, X. Hou, P. Steier, S. Nielsen, R. Golser, Sequential injection method for rapid and
8
9 423 simultaneous determination of ^{236}U , ^{237}Np , and Pu isotopes in seawater. *Anal. Chem.* 85 (2013) 11026-
10
11 424 11033. DOI: 10.1021/ac402673p
- 12
13
14 425 [19] M. Tanimizu, N. Sugiyama, E. Ponzevera, G. Bayon, Determination of ultra-low $^{236}\text{U}/^{238}\text{U}$
15
16 426 isotope ratios by tandem quadrupole ICP-MS/MS. *J. Anal. Atom. Spectrom.* 28 (2013) 1372-1376.
17
18 DOI: 10.1039/C3JA50145K.
- 19 427
20
21
22 428 [20] M. Thirlwall, Inappropriate tail corrections can cause large inaccuracy in isotope ratio
23
24 429 determination by MC-ICP-MS. *J. Anal. Atom. Spectrom.* 16 (2001) 1121-1125. DOI:
25
26 430 10.1039/b103828c
- 27
28
29 431 [21] L. Balcaen, E. Bolea-Fernández, M. Resano, F. Vanhaecke, Inductively coupled plasma-tandem
30
31 432 mass spectrometry (ICP-MS/MS): A powerful and universal tool for the interference-free
32
33 433 determination of (ultra) trace elements-A tutorial review. *Anal. Chim. Acta* 894 (2015) 7-19. DOI:
34
35 10.1016/j.aca.2015.08.053.
- 36 434
37
38
39 435 [22] G. Yang, H. Tazoe, K. Hayano, K. Okayama, M. Yamada, Isotopic compositions of ^{236}U , ^{239}Pu ,
40
41 436 and ^{240}Pu in soil contaminated by the Fukushima Daiichi Nuclear Power Plant accident. *Sci. Rep.* 7
42
43 437 (2017) 13619. DOI: 10.1038/s41598-017-13998-6.
- 44
45
46 438 [23] H. Jaegler, F. Pointurier, S. Diez-Fernández, A. Gourgiotis, H. Isnard, S. Hayashi, H. Tsuji, Y.
47
48 439 Onda, A. Hubert, J.P. Lacey, O. Evrard, Reconstruction of uranium and plutonium dynamics at ultra-
49
50 440 trace concentrations in sediment accumulated in the Mano Dam reservoir, Japan, before and after the
51
52 Fukushima accident. *Chemosphere* 225 (2019) 849-858. doi.org/10.1016/j.chemosphere.2019.03.064
- 53 441
54
55
56 442 [24] A. Gourgiotis, M. Granet, H. Isnard, A. Nonell, C. Gautier, G. Stadelmann, M. Aubert, D.
57
58 443 Durand, S. Legand, F. Chartier, Simultaneous uranium/plutonium separation and direct isotope ratio
59
60
61
62
63
64
65

444 measurements by using CO₂ as the gas in a collision/reaction cell-based MC-ICPMS. *J. Anal. Atom.*
1
2 445 *Spectrom.* 25 (2010) 1939–1945. DOI: 10.1039/c0ja00092b.
3
4
5 446 [25] S.D. Tanner, C. Li, V. Vais, I. Barano, D.R. Bandura, Chemical resolution of Pu(+) from U(+)
6
7 447 and Am(+) using a band-pass reaction cell inductively coupled plasma mass spectrometer. *Anal.*
8
9 448 *Chem.* 76 (2004) DOI : 3042-3048. 10.1021/ac049899j.
10
11
12 449 [26] V. Vais, C. Li, R.J. Cornett, Separation of plutonium from uranium using reactive chemistry in a
13
14 450 bandpass reaction cell of an inductively coupled plasma mass spectrometer. *Anal. Bioanal. Chem.* 380
15
16 451 (2004) 235-239. DOI: 10.1007/s00216-004-2673-3
17
18
19 452 [27] A. Gourgiotis, H. Isnard, M. Aubert, E. Dupont, I. AlMahamid, G. Tiang, L. Rao, W. Lukens, P.
20
21 453 Cassette, S. Panebianco, A. Letourneau, F. Chartier, Accurate determination of Curium and
22
23 454 Californium isotopic ratio by inductively coupled plasma quadrupole mass spectrometry (ICP-QMS)
24
25 455 in ²⁴⁸Cm samples for transmutation studies. *Int. J. Mass Spectrom.* 291 (2010) 101-107.
26
27 456 <https://doi.org/10.1016/j.ijms.2010.02.002>.
28
29
30
31 457 [28] W. A. Russell, D. A. Papanastassiou, T. A. Tombrello, Ca isotope fractionation on the Earth and
32
33 458 other solar system materials. *Geochim. Cosmochim. Acta* 42 (1978) 1075–1090. DOI: 10.1016/0016-
34
35 459 7037(78)90105-9.
36
37
38
39 460 [29] J. Kragten, Calculating standard deviations and confidence intervals with a universally applicable
40
41 461 spreadsheet technique. *Analyst* 119 (1994) 2161-2165. DOI: 10.1016/0169-7439(95)80042-8.
42
43
44 462 [30] J. Kragten, A standard scheme for calculating numerically standard deviations and confidence
45
46 463 intervals. *Chemom. Intell. Lab. Syst.* 28 (1995) 89-97. DOI: 10.1016/0169-7439(95)80042-8.
47
48
49 464 [31] S.D. Tanner, V.I. Baranov, D.R. Bandura, Reaction cells and collision cells for ICP-MS: a tutorial
50
51 465 review. *Spectrochim. Acta, Part B* 57 (2002) 1361-1452. DOI: 10.1016/S0584-8547(02)00069-1.
52
53
54 466 [32] S.F. Boulyga, K.G. Heumann, Determination of extremely low ²³⁶U/²³⁸U isotope ratios in
55
56 467 environmental samples by sector-field inductively coupled plasma mass spectrometry using high-
57
58
59
60
61
62
63
64
65

468 efficiency sample introduction. J. Environ. Radioact. 88 (2006) 1-10. DOI:

1
2
3
4
5
6
7
8
9
10
11
12
13
14
15
16
17
18
19
20
21
22
23
24
25
26
27
28
29
30
31
32
33
34
35
36
37
38
39
40
41
42
43
44
45
46
47
48
49
50
51
52
53
54
55
56
57
58
59
60
61
62
63
64
65

469 10.1016/j.jenvrad.2005.12.007.

470 [33] I.W. Croudace, P.W. Warwick, D.G. Reading, B.C. Russell, Recent contributions to the rapid
471 screening of radionuclides in emergency responses and nuclear forensics. Tr. Anal. Chem. 85 (2016)
472 120–129. DOI: 10.1016/j.trac.2016.05.007.

473

474

475

476

477

478

479

480

481

482

483

484

485

486

487

488

489

490 **Figures and captions**

1
2
3 491 **Figure 1:** Reaction profile of $^{236}\text{U}^{16}\text{O}^+$ in counts.s⁻¹ in MS/MS and mass-shift mode versus O₂ and CO₂
4
5 492 gas flow rates expressed in % of gas in the cell. The concentration of U in solution was 0.050 µg mL⁻¹
6

7
8 493 **Figure 2:** Spectra of a natural U solution at 500 ng mL⁻¹ in SQ mode (a) and in MS/MS mode (b)
9

10 494
11
12 495 **Figure 3:** $^{236}\text{U}/^{238}\text{U}$ isotope ratios obtained by ICP-MS/MS for the non-treated standards (black
13
14 496 squares) and the treated standards (white squares). Black and dotted lines indicate the average value
15
16 497 and the uncertainty range respectively for the non-treated standards. The uncertainties were calculated
17
18 498 according to the Kragten method [27, 28] considering all the sources
19
20

21 499 **Figure 4:** Blank average count rate (counts.s⁻¹) for $^{236}\text{U}^{16}\text{O}^+$ during the analytical sessions. The black
22
23 500 squares represent measurement of instrumental blanks, while the measurement of procedural blanks
24
25 501 are represented by white squares
26
27

28
29 502 **Table 1:** Sensitivity (counts.s⁻¹ for $^{238}\text{U}^{16}\text{O}^+$) and U oxide hydride rates obtained using different
30
31 503 desolvating systems
32

33
34 504 **Table 2:** $^{236}\text{U}/^{238}\text{U}$ isotope ratios measured for the standard IRMM 184. Uncertainties are combined
35
36 505 expanded (k=2) uncertainties calculated according to the Kragten method
37
38

39 506 **Table 3:** $^{236}\text{U}/^{238}\text{U}$ isotope ratios measured for the standard IRMM 075/5. Uncertainties are combined
40
41 507 expanded (k=2) uncertainties calculated according to the Kragten method
42
43

44 508 **Table 4:** Evaluation of the relative contribution (%) of the different sources of errors on the final
45
46 509 uncertainty of the $^{236}\text{U}/^{238}\text{U}$ ratio in IRMM 075/5 (I). Annotation (B) indicates that the counting
47
48 510 corresponds to a blank solution
49
50

51
52 511 **Table 5:** U isotope ratios obtained for the FDNPP samples including the associated combined
53
54 512 expanded uncertainty (k=2). †Measurements by MC-ICP-MS. ‡Measurements by ICP-MS/MS
55
56

57 513 **Figure S1:** Schematic diagram of the chemical treatment and chemical purification protocol of
58
59 514 environmental Fukushima samples
60
61

515 **Table S1:** ICP-MS/MS and MC-ICP-MS operating conditions and acquisition parameters

516 **Table S2:** m/z transitions considered for ICP-MS/MS measurements

517 **Table S3:** Experimental conditions applied for the desolvating systems

518 **Figure S2:** Variation in the $^{238}\text{UO}^+$ intensity ($\text{count}\cdot\text{s}^{-1}$) when adding He. Reaction gases O_2 and CO_2

519 were at 5% and 10% respectively. Helium flux was increased from 0 to 6 mL min^{-1} , by steps of 0.2 mL

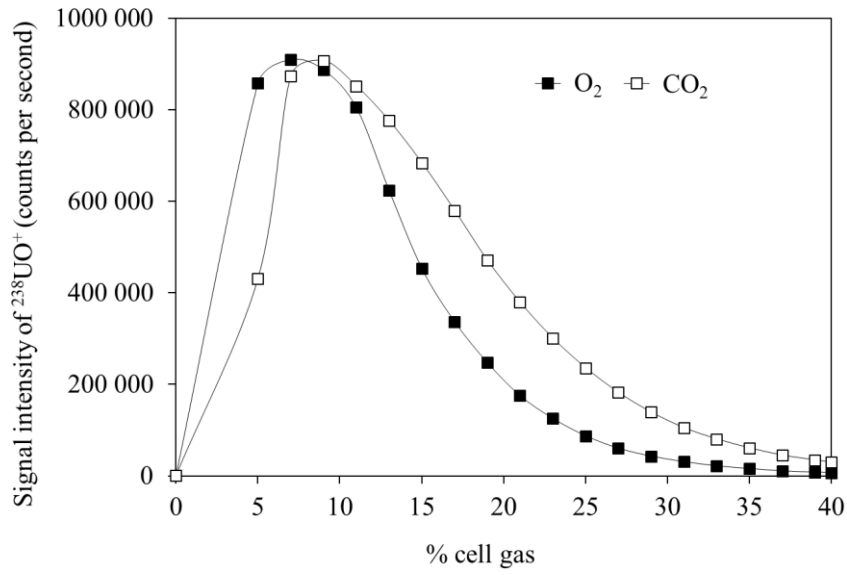
520 min^{-1}

521

522 **Figures**

523 **Figure 1.**

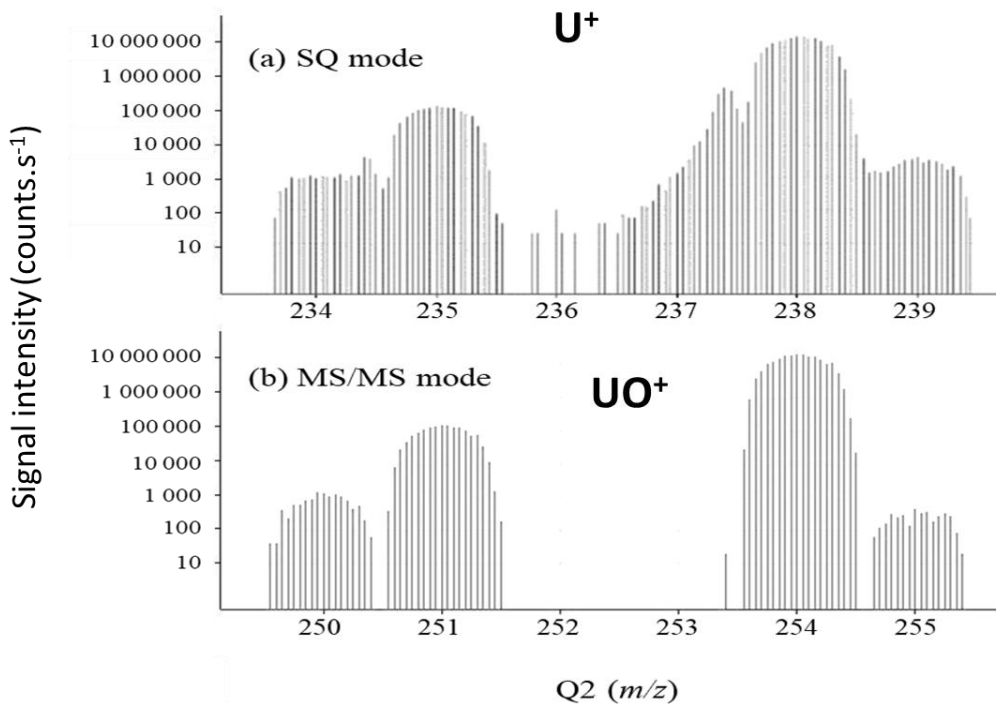
524



525

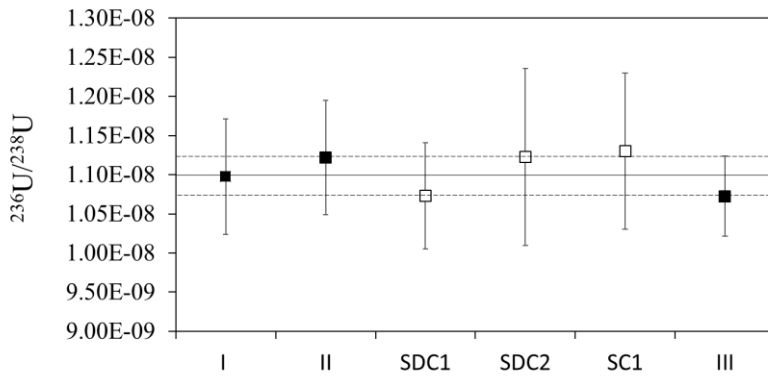
526

527 **Figure 2.**



528

529 **Figure 3.**



530

531

532

533

534

535

536

537

538 **Figure 4.**

539

540

541

542

543

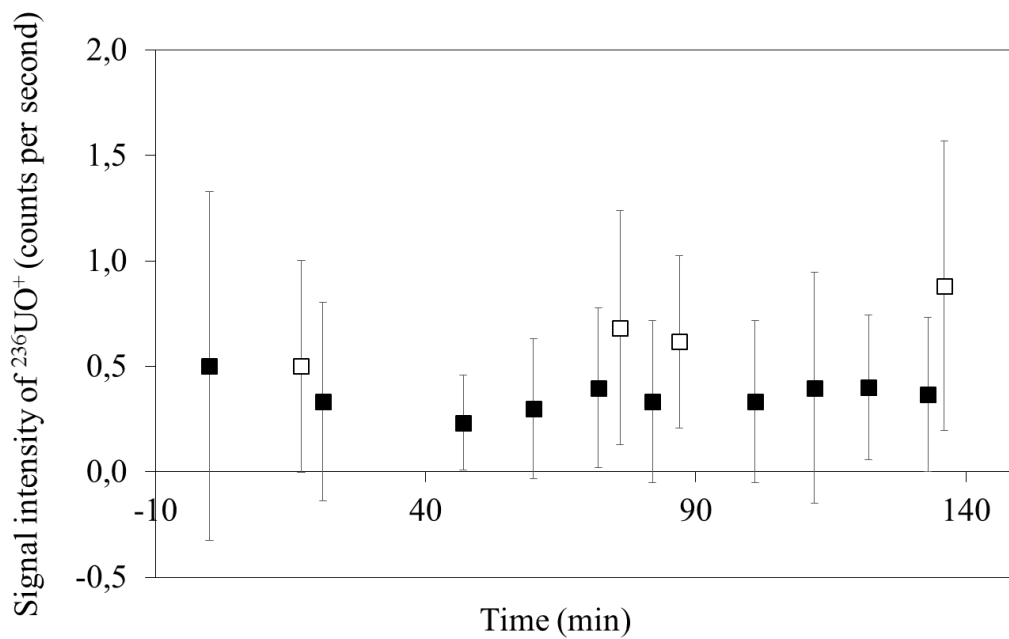


Table 1.

	Standard configuration	Apex IR	Apex HF	Apex HF + Spiro	Apex Ω	Aridus
Sensitivity $^{238}\text{U}^{16}\text{O}^+$ counts.s⁻¹ per ng mL⁻¹	90 000 – 110 00	110 000 – 150 000	220 000 – 280 000	~250 000	400 000 – 600 000	400 000 – 600 000
Hydride rate ($^{238}\text{U}^{16}\text{O}^1\text{H}^+ / ^{238}\text{U}^{16}\text{O}^+$)	3×10^{-6}	3×10^{-6}	3×10^{-6}	4×10^{-6}	4×10^{-7}	4×10^{-7}

542 **Table 2.**

543

Standard IRMM 184	$^{236}\text{U}/^{238}\text{U}$	Combined expanded uncertainty	Relative combined expanded uncertainty (%)	Relative difference/certified ratio %
Certified ratio	1.2446×10^{-7}	0.0017×10^{-7}	0.13	
I	1.239×10^{-7}	0.039×10^{-7}	3.2	-0.4
II	1.216×10^{-7}	0.040×10^{-7}	3.3	-2.3
III	1.241×10^{-7}	0.025×10^{-7}	2.0	-0.3
IV	1.251×10^{-7}	0.025×10^{-7}	2.0	0.5
V	1.207×10^{-7}	0.022×10^{-7}	1.8	-3.0
VI	1.252×10^{-7}	0.028×10^{-7}	2.2	0.6
VII	1.250×10^{-7}	0.028×10^{-7}	2.2	0.5
Average ratio	1.237×10^{-7}			
StdDev (n=7)	0.018×10^{-7}			
Relative StdDev (%)	1.5			
Relative difference/ certified ratio (%)	-0.6			

544

545

546 **Table 3.**

Standard IRMM 075/5	$^{236}\text{U}/^{238}\text{U}$	Combined expanded uncertainty	Relative combined expanded uncertainty (%)	Relative difference / certified ratio %
Certified ratio	1.06519x10 ⁻⁸	0.00075x10 ⁻⁸	0.07	6.3
I	1.13x10 ⁻⁸	0.15x10 ⁻⁸	13.5	6.3
II	1.10x10 ⁻⁸	0.09x10 ⁻⁸	8.3	3.4
III	1.04x10 ⁻⁸	0.09x10 ⁻⁸	8.7	-2.0
IV	1.14x10 ⁻⁸	0.11x10 ⁻⁸	9.5	7.3
V	1.19x10 ⁻⁸	0.10x10 ⁻⁸	8.3	8.3
VI	1.04x10 ⁻⁸	0.24x10 ⁻⁸	22.8	-2.8
VII	1.00x10 ⁻⁸	0.20x10 ⁻⁸	19.4	-5.6
Average ratio	1.09x10⁻⁸			
StdDev (n=7)	0.068x10⁻⁸			
Relative StdDev (%)	6.2			
Relative difference / certified ratio (%)	2.3			

36 548

39 549

41 550

1
2
3
4
5
6 551
7
8
9 552
10
11
12
13
14
15
16 553
17
18 554
19
20
21 555
22
23
24
25
26
27
28
29
30
31
32
33
34
35
36
37
38
39
40
41 556
42
43
44
45
46
47
48
49

Table 4.

Source of uncertainty	$^{234}\text{UO}^+$ cps (B)	$^{234}\text{UO}^+$ cps	$^{235}\text{UO}^+$ cps (B)	$^{235}\text{UO}^+$ cps	$^{236}\text{UO}^+$ cps (B)	$^{236}\text{UO}^+$ cps	$^{238}\text{UO}^+$	$^{238}\text{U}^1\text{H}^+$ cps	$^{234}\text{U}/^{235}\text{U}$ ref	$^{235}\text{U}/^{238}\text{U}$ ref
Contribution (%)	0.65	<0.0001	1.10	<0.0001	90.7	0.44	0.12	6.61	0.35	0.001

Table 5.

Sample	$^{235}\text{U}/^{238}\text{U}^\dagger$	Combined expanded uncertainty	$^{234}\text{U}/^{235}\text{U}^\dagger$	Combined expanded uncertainty	$^{236}\text{U}/^{238}\text{U}^\ddagger$	Combined expanded uncertainty	Relative combined expanded uncertainty (%)
MDh	0.007257	0.000002	0.008296	0.000008	1.64×10^{-8}	0.11×10^{-8}	6.7%
MD1	0.007253	0.000002	0.008379	0.000009	2.42×10^{-8}	0.36×10^{-8}	14.9%
MD2	0.007256	0.000002	0.008141	0.000008	1.20×10^{-8}	0.20×10^{-8}	16.6%
MD3	0.007258	0.000002	0.008077	0.000008	8.93×10^{-9}	1.5×10^{-9}	16.8%
MDp	0.007261	0.000002	0.007955	0.000009	6.94×10^{-9}	1.1×10^{-9}	15.9%
MD4	0.007258	0.000002	0.008277	0.000009	1.49×10^{-8}	0.15×10^{-8}	10.1%
MDb	0.007255	0.000002	0.008078	0.000008	7.19×10^{-9}	0.84×10^{-9}	11.7%

Supplementary Material

[Click here to download Supplementary Material: Supplementary Information.docx](#)

